ORIGINAL PAPER

Climatic variability of river outflow in the Pantanal region and the influence of sea surface temperature

Carlos Batista Silva[1] · Maria Elisa Siqueira Silva[1] · Tércio Ambrizzi[2]

Abstract This paper investigates possible linear relationships between climate, hydrology, and oceanic surface variability in the Pantanal region (in South America's central area), over interannual and interdecadal time ranges. In order to verify the mentioned relations, lagged correlation analysis and linear adjustment between river discharge at the Pantanal region and sea surface temperature were used. Composite analysis for atmospheric fields, air humidity flux divergence, and atmospheric circulation at low and high levels, for the period between 1970 and 2003, was analyzed. Results suggest that the river discharge in the Pantanal region is linearly associated with interdecadal and interannual oscillations in the Pacific and Atlantic oceans, making them good predictors to continental hydrological variables. Considering oceanic areas, 51 % of the annual discharge in the Pantanal region can be linearly explained by mean sea surface temperature (SST) in the Subtropical North Pacific, Tropical North Pacific, Extratropical South Pacific, and Extratropical North Atlantic over the period.

Considering a forecast approach in seasonal scale, 66 % of the monthly discharge variance in Pantanal, 3 months ahead of SST, is explained by the oceanic variables, providing accuracy around 65 %. Annual discharge values in the Pantanal region are strongly related to the Pacific Decadal Oscillation (PDO) variability (with 52 % of linear correlation), making it possible to consider an interdecadal variability and a consequent subdivision of the whole period in three parts: 1st (1970–1977), 2nd (1978–1996), and 3rd (1997–2003) subperiods. The three subperiods coincide with distinct PDO phases: negative, positive, and negative, respectively. Convergence of humidity flux at low levels and the circulation pattern at high levels help to explain the drier and wetter subperiods. During the wetter 2nd subperiod, the air humidity convergence at low levels is much more evident than during the other two drier subperiods, which mostly show air humidity divergence. While the drier periods are particularly characterized by the strengthening of northerly wind over the center of South America, including the Pantanal region, the wetter period is characterized by its weakening. The circulation pattern at 850 hPa levels during the drier subperiods shows anticyclonic anomalies centered over east central South America. Also, the drier subperiods (1st and 3rd) are characterized by negative stream function anomalies over southeastern South America and adjacent South Atlantic, and the wetter subperiod is characterized by positive stream function anomalies. In the three subperiods, one can see mean atmospheric patterns associated with Rossby wave propagation coming from the South Pacific basin—similar to the Pacific South America pattern, but with reverse signals between the wetter and the drier periods. This result suggests a possible relationship between climatic patterns over southeastern South America regions and the Pacific conditions in a decadal scale.

✉ Carlos Batista Silva
krlosbatist@gmail.com

✉ Maria Elisa Siqueira Silva
elisasiq@usp.br

✉ Tércio Ambrizzi
ambrizzi@model.iag.usp.br

[1] Department of Geography, College of Philosophy, Letters and Human Sciences, University of São Paulo, Av. Prof. Lineu Prestes,338, Cid. Universitária, São Paulo, SP, Brazil

[2] Department of Atmospheric Sciences, Institute of Astronomy, Geophysics and Atmospheric Sciences, University of São Paulo, Rua do Matão, 1226, Cid. Universitária, São Paulo, SP, Brazil

1 Introduction

Sea surface temperature is an important atmospheric forcing (e.g., Walker 1924; Bjerknes 1969; Hoskins and Karoly 1981; Müller and Ambrizzi 2007), being able to modify global atmospheric flow patterns, which result in pressure and wind fields changes through Rossby wave propagation. Several studies have pointed out the association between modified atmospheric fields and oceanic variability, particularly over the Equatorial Pacific (Kousky et al. 1984; Rao et al. 1986; Ropelewski and Halpert 1989). One important aspect is the influence of sea surface temperature (SST) anomalies on precipitation and continental air temperature behavior over South America (Aceituno 1988; Uvo et al. 1998; Rao and Hada 1990; Coelho et al. 2002; Taschetto and Ambrizzi 2012; Saji et al. 2005; Drumond and Amrbizzi 2005; Drumond and Ambrizzi 2008) and on river discharge (Aceituno 1988; Genta et al. 1998; Camilloni and Barros 2000).

The SST association with river discharge variability in South America was verified by Robertson and Mechoso (1998) in which four important rivers were considered, Negro, Uruguay, Paraguay, and Paraná. Besides linear tendency, the authors observed interannual (3, 5, and 6 years) and quasi-decadal (9 years) periodicities in the discharge time series. Negro and Uruguay discharges data showed more intense interannual cycles, while Paraguay and Paraná discharges were more closely related to quasi-decadal variability. The first two rivers were mostly associated with ENSO (El Niño/ Southern Oscillation) variability, while the last two were associated with tropical North Atlantic variability. ENSO is an important interannual oscillation pattern over the Tropical Pacific Ocean, indicated through SST anomalies and climatic indices (Bjerknes 1969; Quinn et al. 1978; Quinn and Neal 1984, 1985; Trenberth 1984; Trenberth 1997; Trenberth and Hoar 1996, 1997; Kiladis and van Loon 1988; Nitta and Yamada 1989; McPhaden 2002). ENSO may impact many regions around the world, particularly with changes in precipitation and air temperature. Cardoso and Silva Dias (2006) observed analogous results when analyzing river discharge data over the State of São Paulo, in southeastern South America, in association with the Pacific (160°–90° W; 25°– 35° S) and the Atlantic (40°–0° W; 30°–40° S) SST. They showed that the Pacific SST has more significant linear correlation in interannual time scale, while the Atlantic SST is more related to a decadal time scale. Analyzing the climate variability for the same rivers studied by Robertson and Mechoso (1998); Genta et al. (1998) observed changes in average values of discharge time series before and after the decade of 1970. Niño1 + 2 SST, at the Equatorial Pacific Ocean, as pointed out by the authors, influenced this change. In fact, SST anomalies from Niño1 + 2 and Niño3 regions seem to influence significantly the river discharge behavior in areas located in the central-south region of Brazil, as

discussed in Cardoso et al. (2004). In this case, the authors mention significant influence in the discharge data up to 4 months after SST observations.

The relationship between Pacific SST and river discharge over South America was studied by Camilloni and Barros (2000). In this work, they tried to better understand the physical causes of discharge anomalies associated with two El Niño events of similar intensities, 1982–1983 and 1997– 1998. Although El Niño intensities were similar, the responses in the Paraná River discharge in the Argentinean region were very different in both events. The river discharges during the 1982–1983 El Niño were greatly more expressive than observed during the 1997–1998 event. Camilloni and Barros (2000) suggested that the atmospheric convection patterns formed over the Paraná basin during the two events were distinct from each other. In addition, the highest linear correlation values between SST and Paraná discharge data, during the 1982–1983 El Niño, were found in the Niño3 SST region, while in the 1997–1998 event, the highest correlation values occurred over Niño1 + 2. This result suggests how the positioning of heat forcing over the oceans can influence spatially the variability of remote climate systems (Drumond and Ambrizzi 2003; Magaña and Ambrizzi 2005). Besides the Pacific influence, Camilloni and Barros (2000) also indicated high and significant correlation (~0.4) of SST in South Atlantic areas, between 10° S–30° S and to east of 20° W, during both El Niño events.

In general, the central part of South America is characterized as a transition area between subtropical and tropical climate, where climate predictability is weak (Fernandez et al. 2006), and there are few studies focused on this region. The Pantanal region is located in the central part of South America (between 58° W; 16° S, and 50° W; 20° S, upper stream of Paraguay River), occupying vast plains in the Brazilian territory. It is known as the greatest flooding area in the world (Pinto 1988), having a total extent of 367,227 km^2. Its geomorphological and hydrological characteristics make it a regulator of the water regime, by acting as a "sponge" and delaying the water flow (Souza et al. 2006). The delaying characteristic is essential for the Paraguay River natural discharge control, influencing the electrical power generation, navigation, urban supply, and crop irrigation over part of Brazilian, Argentine, and Paraguayan territories. The delay process is also important to keep fauna and flora in this biome (Ab'Saber 1939). Partially due to the delay process, it is considered as the most vulnerable Brazilian biome (Ab'Saber 1939 and Souza et al. 2006). Thus, a better understand of the characteristics of climatic variability in the Pantanal region is fundamental for territorial economic planning of the regions in the Southern Cone of the South American continent.

The main objective of the present study is to analyze the climate and hydrology variability over central South America (SA), more specifically in the Pantanal region and its

relationship with oceanic areas. In this study, stochastic models for the Pantanal discharge, through linear correlation and regression analysis, are proposed. Also, climatic atmospheric patterns are considered in order to better understand the characteristic atmospheric conditions related to wetter and drier periods over central SA.

2 Data and Methods

Association between river discharge in the Pantanal basin and SST over the global oceans has followed three steps: linear correlation between the two variables; construction of linear stochastic models for river discharge, considering SST and climate indices as independent/predictors variables; and analysis of atmospheric patterns, including the Pacific Decadal Oscillation, in order to verify possible physical associations.

River discharge data for the entire Pantanal basin was obtained for the 1970–2003 period, in monthly scale, from Agência Nacional de Águas—ANA (Brazilian Water National Agency), governmental administration responsible for hydrological resources regulation in Brazil (available at <http://hidroweb.ana.gov.br/>). The lack of data in several stations had constrained the choice of larger time series. The rivers considered in this study are Cuiabá, Miranda, Aquidauana, Itiquira-Piquiri, Taquari, and São Lourenço, of which the basic hydrography is shown in Fig. 1. Hydrography indicates all the rivers flowing from east-northeast to west sectors, following the topography of the Brazilian central highlands. Monthly SST dataset was obtained from NOAA (National Oceanic and Atmospheric Administration; <http://www.esrl.noaa.gov/psd/data/gridded/data.kaplan_sst.html>) with 5 degrees of spatial resolution. A full description of NOAA's SST dataset characteristics is given in Kaplan et al. (1998). Precipitation data were obtained from the University of Delaware (named here as LW; <http://www.esrl.noaa.gov/psd/data/gridded/data.UDel_AirT_Precip.htm>) and presents 0.5 degree of spatial resolution for the period 1900–2010, as described in Legates and Willmott (1990).

Some climate indices, such as the Pacific Decadal Oscillation (PDO, Latif and Barnett 1994, 1996; Hare and Francis 1995; Mantua et al. 1997; Minobe 1997; Zhang et al. 1997; Gershunov and Barnett 1998; Mantua and Hare 2002) and SST for the Niño regions (Niño1 + 2, Niño3.4, Niño3, and Niño4), obtained from NOAA (<http://www.esrl.noaa.gov/psd/data/climateindices/list/>), are used as possible predictors for further statistical modeling. ENSO characterization is commonly drawn from climatic indices defined by SST anomalies in specific areas over equatorial Pacific.

Cluster analysis (Wilks 1995) was applied to the six Pantanal discharge time series to verify climatic spatial homogeneity among the considered stations. Results showed two main distinct groups: one composed solely by the Miranda

River time series (river 6, in Fig. 1), and the other composed by the remaining five time series, Cuiabá, Aquidauana, São Lourenço, Itiquira-Piquiri, and Taquari (rivers 1 to 5, in Fig. 1). Based on the cluster analysis, this study will consider only the second group, represented by the average among them, called henceforth Pantanal discharge.

To identify key oceanic areas associated with river discharge in Pantanal, monthly linear correlation was calculated. Both SST and discharge data were smoothed by 12-month running mean. The 12-month running mean smoothening provides higher spatial confidence in the signal obtained for correlation calculus (over the ocean) in comparison to the one obtained from the original data. Although this assumption weakens the linear relation between river discharge and SST in seasonal scale, it can be useful for climatic purposes, occasionally providing significance to enlarged continental areas in which climate can partially be influenced by particular oceanic portions. Linear correlation was computed with and without monthly lag between SST and river discharge, up to 9 months, as shown in Eq. 1. Considering the prediction prognostic purpose, discharge time series were always displaced ahead of the SST time series. In the correlation analysis, January was considered as the initial month for the SST time series. The other months of the year (February to December) were also considered in the correlation, showing similar results to those obtained for January, therefore not being shown in this study.

$$r_{i,p} = \frac{\left(x_i - \overline{x}\right)\left(y_{i+p} - \overline{y}\right)}{S_{xx}S_{yy}}, \quad p = [0, 8] \text{ and } i = [1, 11] \quad (1)$$

where i represents the x temporal variation and p, the y variation; x and y represent SST and river discharge variables. $\overline{x}$ and $\overline{y}$ represent the respective means for the whole period. S_{xx} and S_{yy} represent the standard deviation for x and y variables.

Seasonality and linear tendency were removed from the time series before any correlation calculation, and the time series values were normalized by the standard deviation. Linear trend was removed from the original data in order to emphasize "natural" climatic variability. Statistical significance for linear correlation coefficients was considered above 99 % by the application of Student t test. Spatial mean SST values from higher correlated areas to the Pantanal river discharge were considered as potential predictors in the construction of stochastic models for the Pantanal river discharge simulation and prediction. The five SST areas retained in the stochastic models are presented in Fig. 2a.

The construction of stochastic models for river discharge simulation in the Pantanal basin was based on multiple linear regressions (Wilks 1995). The models were constructed in annual and monthly scales and for diagnostic and predictive purposes. In the prediction case, a temporal lag of 3 and
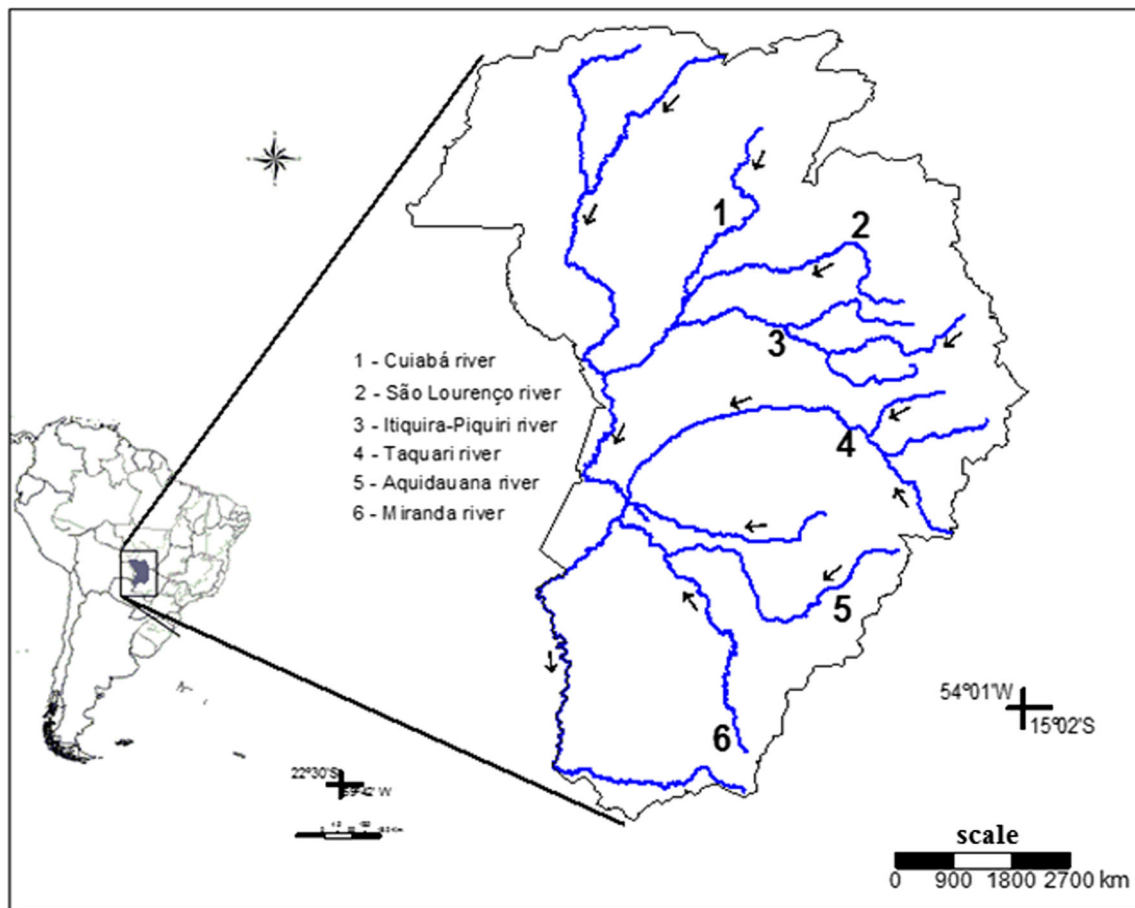
Fig. 1 Pantanal hydrological basin in South America and location of the rivers in the basin: *1* Cuiabá, *2* São Lourenço, *3* Itiquira-Piquiri, *4* Taquari, *5* Aquidauana, and *6* Miranda. *Arrows* indicate the stream direction

6 months between independent variables and the Pantanal discharge was considered. Linear adjustment was constructed under backward stepwise processes with the statistical R-package. Prediction verification was estimated through the mean absolute error (MAE), described by Willmott and Matsuura (2005) as

$$MAE = \frac{1}{n} \sum\nolimits_{i=1}^{n} \frac{|P_i - O_i|}{|O_i|} \qquad (2)$$

where P_i and O_i are predicted and observed data and n represents the number of elements in the times series.

In order to identify the characteristic patterns during periods of distinct river discharge anomalies in the Pantanal basin, anomalous fields for divergence of humidity flux at low levels (from 1000 to 700 hPa), vector wind at 850 hPa, smoothened geopotential height and stream function at upper levels (250 hPa and 0.21 sigma level, respectively) were used. Geopotential height and stream function were filtered to capture the low frequency sign; the interannual frequency (low-pass) was selected using a Lanczos' filter (Duchon 1979). Atmospheric data were obtained from the Reanalysis I dataset (Kalnay et al. 1996). To capture the main features of

the rainy season at the studied region, all climatic fields were analyzed from October to March—being this definition of rainy season in the region used by various other authors (Zhou and Lau 1998; Vera et al. 2006; Rao and Hada 1990; Pinheiro et al. 2002).

3 Results

Results are presented in two sections, the first focusing on stochastic modeling proposition, based on linear correlation and regression analysis, and another investigating the climatic patterns related to drier and wetter subperiods for discharges values in the Brazilian Pantanal region.

3.1 Stochastic modeling approach for seasonal Pantanal river discharge

Important areas over the Pacific and Atlantic oceans are well correlated to Pantanal river discharge in the period of 1970–2003, as seen in Fig. 2, with absolute values as high as 0.6 (colored areas have statistical significance higher than 99 %).

Fig. 2 Lagged linear correlation between Pantanal discharge and SST monthly data for the period of 1970–2003, for **a** lag = 0, **b** lag = 4, **c** lag = 8, and **d** lag = 11 months. The first month in SST time series is always January. The five areas (depicted in *black rectangles*) over the Pacific and the Atlantic oceans used as independent variables in the linear adjustment are Subtropical North Pacific (*1*), Tropical North Pacific (*2*), Extratropical South Pacific (*3*), Southeast South Atlantic (*4*), and Extratropical North Atlantic (*5*). The statistical significant areas at 99 % (Student *t* test) are given by *black lines* ($t_c \geq 0.2$)
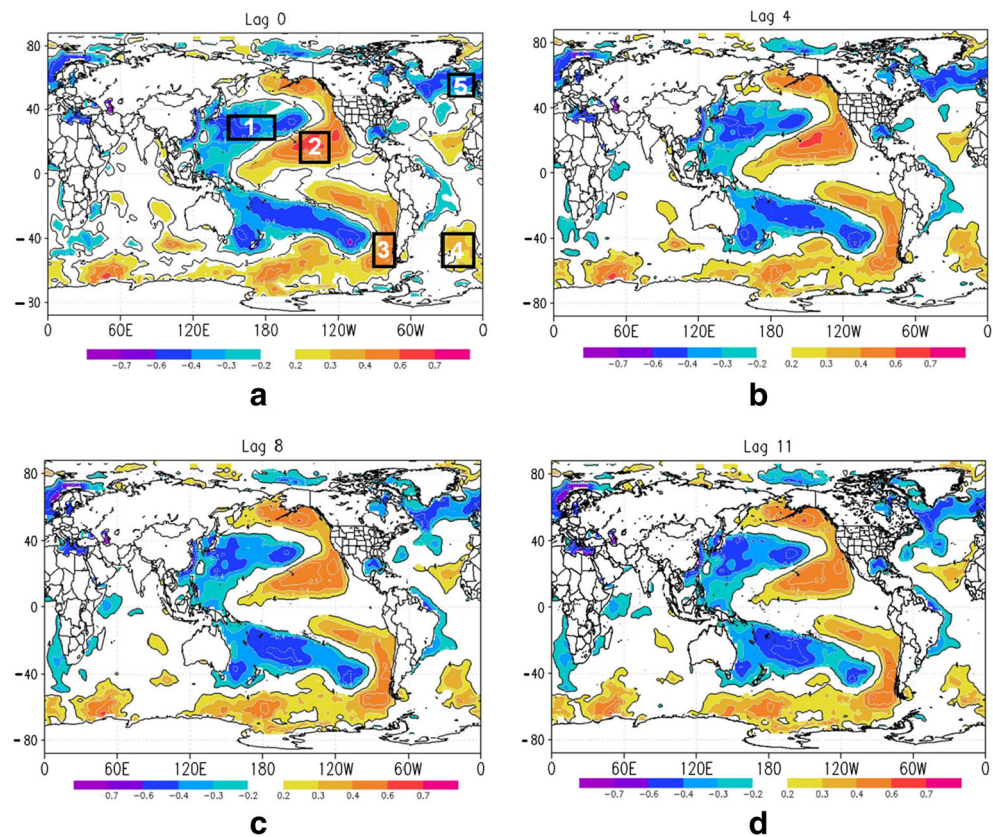
In the Pacific and Atlantic oceans, correlations between SST and Pantanal river discharge show positive and negative values. Previous studies (Deser et al. 2010; Cardoso and Silva Dias 2006; Kawamura 1994; Weare et al. 1976) have already shown that the areas depicted in Fig. 2 are well correlated with South America hydrological variables, showing their importance in EOF analysis. The spatial pattern obtained from this calculation over the Pacific basin presents high spatial homogeneity and a "horseshoe" shape, similar to the first SST EOF mode shown in Kao and Yu (2009), indicating PDO association (Trenberth and Stepaniak 2001). Negative and positive correlation values are observed from west to east sectors of the Pacific basin (Fig. 2a), respectively.

It is also noted that the correlation values over subtropical and tropical regions at the North Pacific (both for negative and positive values) present higher absolute values than those located over the South Pacific at the same latitude belts. Over subtropical areas of North Pacific, close to 160° W and 20° N, the highest positive values range from 0.6 to 0.7. On the other hand, at a symmetric location in the South Pacific, the highest positive values range from 0.3 to 0.5. The areas characterized by negative correlation, in subtropical latitudes, present the highest absolute values ranging from −0.6 to −0.5 in the North Pacific and −0.3 to −0.5 in the subtropical South Pacific. The spatial pattern remains almost unchangeable for lagged correlation, as seen from frames (b) to (d) of Fig. 2. The

spatial similarity in the correlation computation for different lags can be caused by different reasons: specific climatic sensitivity of the Pantanal region in relation to distinct oceanic areas and the considered smoothing. Discussion about the Pantanal discharge in relation to distinct scales, particularly to those smaller than the annual scale, will not be addressed in this study; though, preliminary analysis for river discharge of other regions of South America indicates different results and distinct sensitivity to ocean data for monthly lagged correlation even considering smoothed data. Significant and positive correlation values are seen over South Pacific, further south, between 60° S and 45° S, and 80° W and 100° W, with maximum values ranging from 0.5 to 0.6. The linear correlation pattern obtained for the Pacific basin is also observed in the first SST EOF mode in Deser et al. (2010). Results obtained by Deser et al. (2010) are related to monthly SST from HadlSST dataset (Rayner et al. 2003) for the period of 1900–2008. The similarity between the EOF first mode and the linear correlation spatial pattern obtained in the present study and the results found by Deser et al. (2010) corroborates the interconnection assumption between hydrological and oceanic variability through atmospheric circulation, which can be characterized by climatic patterns, such as ENSO and PDO.

South Atlantic SST also presents significant positive correlation to Pantanal discharge, although smaller than the observed

in the Pacific Ocean. Significant and positive linear correlation values with the Pantanal discharge are seen over the Atlantic southeast region, between 30° S and 60° S, and from 40° W to the Greenwich meridian, with the highest values ranging from 0.4 to 0.5. The linear correlation pattern observed in the South Atlantic is similar to the spatial pattern obtained by Cardoso and Silva Dias (2006), who applied Canonical Correlation Analysis in monthly SST and Paraná river discharge, between 1950 and 2001. High and negative SST correlation signals in the North Atlantic Ocean appears to the north of 50° N, with absolute values greater than 0.6.

Linear correlation between climate indices and the rivers discharge time series is presented in Table 1. Highest correlation values occur for PDO and SOI indices. Besides PDO, Niño regions also appear to be important for the Pantanal discharge variability. Castillo et al. (2014) contributed to the understanding of how moisture transport from oceanic sources occurs during ENSO phases. In their study, the authors showed some ENSO influence on moisture transport to the SA central area during summer and autumn. North Atlantic Oscillation (NAO, defined as the difference between surface pressure anomalies over Iceland and Açores in Walker and Bliss (1932); van Loon and Roger (1978); Hurrell (1995)) and Southern Annular Mode (SAM, defined as the difference between sea level pressure anomalies over 40° S e 65° S in and Gong and Wang (1999)) indices seem to be of less importance for the discharge in the Pantanal region. Although NAO is an important climatic oscillation, there are few studies which investigated its association with South America climate. The impact of SAM on SA climate variability is better known, as pointed by Gillett et al. (2006) and Reboita et al. (2009). These two studies indicated that SAM and precipitation variability over SA central areas occur in phases. During negative (positive) SAM phases, the summer and autumn precipitation anomaly over the south-central SA is also negative (null and positive), as pointed by Reboita et al. (2009).

To further analyze possible linear associations between ocean climate variability and river discharge in the Pantanal region, averaged SST values for distinct oceanic areas (as shown in Fig. 2a) were considered as independent variables in a linear approach. Initially, 11 oceanic areas with high correlation absolute values, greater than 0.3 (not shown here), were selected. Statistical significance higher than 99 % occurs when correlation values are greater than 0.3 for these datasets. After applying linear adjustment, only five areas were chosen and considered as predictors in the predictive approach. The five selected oceanic regions (Fig. 2a) used in the diagnostic and predictive models are (1) Subtropical North Pacific (SNP), (2) Tropical North Pacific (TNP), (3) Extratropical South Pacific (ESP), (4) Southeast South Atlantic (SSA), and (5) Extratropical North Atlantic (ENA). The same areas, as indicated in Fig. 2a, were considered for the annual and seasonal scale modeling. The results related to the linear adjustment obtained for annual and seasonal scales, for diagnostic and predictive approaches to Pantanal discharge, will be discussed below. The proposed models were based on SST and river discharge data smoothed by 12 times running mean.

The linear model obtained for annual discharge simulation in the Pantanal region is given by:

$$\text{Annual Pantanal discharge} = 0.051 + 0.523 \times SNP$$
$$+ 0.581 \times TNP + 0.412$$
$$\times ESP - 0.41 \times ENA,$$

where the numbers represent the linear and angular coefficients obtained from the linear adjustment and the acronyms are averaged SST over the considered oceanic areas, as indicated in Fig. 2a. This linear adjustment explains 51 % of the annual discharge variance observed in Pantanal in the period of 1970–2003. Differently, models constructed with original data without smoothening show very poor association between oceanic and discharge variables (with $R^2 \sim 0.048$).

Simulated (black bars) and observed (gray bars) annual values are plotted in Fig. 3. Although there are some differences between annual values, positive and negative variability

Table 1 Linear correlation between monthly discharge in the Pantanal region and climate indices for the period of 1970–2003

River station	PDO	SOI	NAO	SAM	Niño1 + 2	Niño3 + 4	Niño3	Niño4
Pantanal mean								
Aquidauana	0.57*	(−0.40)	0.06	0.02	0.32*	0.3*	0.12	0.07
São Lourenço	0.35*	(−0.10)	(−0.08)	0.11	0.11*	0.08	0.10	0.04
Piquiri-Itiquira	0.56*	(−0.32)*	0.02	(−0.01)	0.22*	0.17*	0.27*	0.22*
Taquari	0.24*	(−0.33)*	0.15	0.18*	0.71*	0.40*	0.58*	0.22*
Cuiaba	0.43*	(−0.28*	0.21*	(−0.03)	0.22*	0.24*	0.23	0.22*
Pantanal	0.43*	(−0.28*)	0.07	0.05	0.3	0.23*	0.2	0.23

PDO pacific decadal oscillation, *SOI* South Oscillation Index, *NAO* North Atlantic Oscillation, *SAM* Southern Annular Mode. *Indicates statistical significance of 95 %
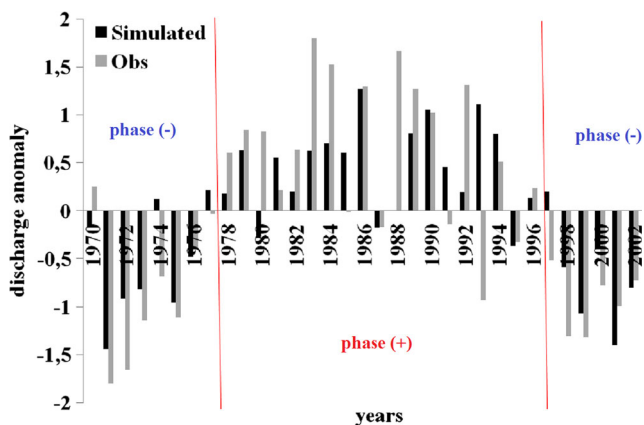
Fig. 3 Simulated (*black bars*) and observed (*gray bars*) normalized discharge anomaly (m^3 s^{-1}) in Pantanal for the period of 1970–2003 by linear regression considering mean SST at SNP, TNP, SSA, ESP, and ENA locations as independent variables. All data were smoothed by a 12-month running mean. The linear adjustment presents R^2 equal to 51 %. *Vertical red lines* in the graph mark the three considered subperiods

patterns, characterized by a temporal scale of 10–20 years, between simulated and observed values are similar. The years 1993 and 1997 present strong differences between observed and simulated signals, approximately 2.3 and 0.7 standard deviation (SD), respectively. The major part of the years showed the same signal for simulated and observed discharges. When separate analysis are considered for each independent variable (SNP, TNP, ESP, and SSA), TNP, and SNP are noticed as the best areas to explain the linear variability of the Pantanal annual discharge. These areas separately explain 33.8 % and 27.3 %, respectively, of the annual discharge, as indicated in Table 2.

Because of the persistent linear spatial patterns in correlation values observed for all temporal lags considered (0–11 months), the performance of a stochastic model for river discharge prediction was tested. All models in monthly scale were constructed with smoothed data by 12-month running mean. The independent variables considered in the monthly model construction were the same as those used in the annual model. The resulting prediction model, in monthly scale, is formed by five independent variables: mean

Table 2 Variance explanation (R^2) for discharge in Pantanal by each SST area: Subtropical North Pacific (SNP), Tropical North Pacific (TNP), Extratropical South Pacific (ESP), Southeast South Atlantic (SSA), and Extratropical North Atlantic (ENA). Data were smoothed by 12-year running mean

Oceanic areas	R^2
SNP	27.3
TNP	33.8
ESP	24.0
SSA	17.0
ENA	16.8

SST at SNP, TNP, SSA, ESP, and ENA locations. The model was developed for the period of 1970–1992 (264 months), and its skill was verified for the remained period, 1993 to 2003 (120 months). The Pantanal mean discharge variances explained by the five independent variables (R^2) in the two prognostic models, for 3 and 6 months in advance, are respectively equal to 68 and 45 %. The adjustment for 3 months ahead in relation to observed data can be seen in Fig. 4, and it is written as

$$\text{Pantanal monthly discharge}(t) = 0.047 + 0.084*TNP(t{-}3)$$
$$+ 0.116*SNP(t{-}3)$$
$$+ 0.155*SSA(t{-}3){-}0.100*ENA(t{-}3)$$
$$+ 0.274*ESP(t{-}3),$$

where t is the month for which the prediction is made, the numbers represent linear and angular coefficients obtained in the linear adjustment and the acronyms are averaged SST over the considered oceanic areas indicated in Fig. 2a. While the annual linear regression selected four independent variables, the month approach considered all five independent variables. Mean SST in the Extratropical North Atlantic is the required additional variable in the month approach that explains ~17 % of the discharge variance.

The result between predicted and observed monthly river discharges is in relative good agreement, as seen in Fig. 5. This figure depicts the simulated discharge 3 and 6 months ahead the SST values and the observed values. The mean errors for the 3- and 6-month forecasting period, defined between 1993 March (1993 July, in the case of 6 months ahead) and 2003 December, are equal to 34.5 and 34.7 %, respectively, providing significant accuracy degrees of 65.5 and 65.3 %. Applying a linear adjustment between 3 months ahead predicted and observed discharge, the mean error becomes equal to 27 % (figure not shown). The stochastic model seems to
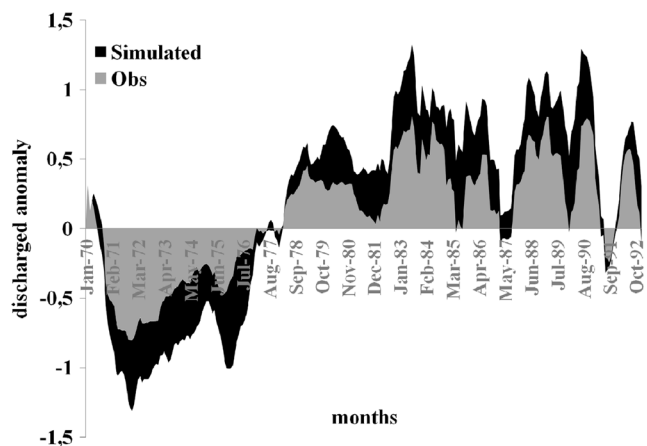

Fig. 4 Simulated (*black*) and observed (*gray*) monthly normalized discharge anomaly (m^3 s^{-1}) (3 months ahead) in the Pantanal region. The linear model was built for the period of 1970 January–1992 December and explains 68 % of the observed variance
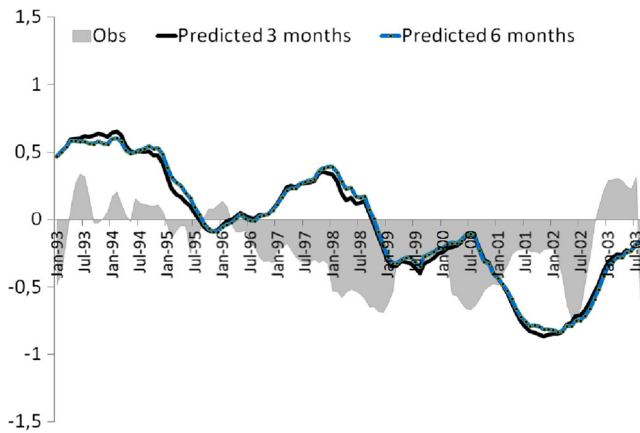
Fig. 5 Predicted for 3 and 6 months ahead (*black and blue lines*) and observed (*gray bars*) monthly anomaly discharge in Pantanal between 1993 March (July, for 6 months ahead) and 2003 December. Mean errors are respectively equal to 34.5 and 34.7 %

represent mostly interdecadal variability, as shown by positive prognostic discharge anomalies simulated for the first half of the prognostic period (Fig. 5), up to 1998 July, and negative anomalies during the last half of the time series. As the linear correlation between SST and the Pantanal river discharge should only capture the linear signal, linear models constructed under this assumption will mostly explain the linear relations between dependent and independent variables. Particularly, both prognostic models misrepresent the discharge predicted on the period between 1996 August and 1998 September, as shown in Figs. 5 and 6. During this period, the South Atlantic and the South Pacific SST, SSA, and ESP areas do not show linear relation to discharge in the Pantanal region, providing the misrepresentation by the linear model. Data smoothening is another point that helps to explain some weakness in the proposed models. The 12-month running mean assumption should remove part of the seasonal sign. This means the selected independent variables by the stochastic processes are more related

to interannual or lower scales variability, providing better models for smoother data. Even so, the proposed models for seasonal scale present relatively high accuracy degree (∼ 65 %), as previously mentioned.

3.2 General atmospheric patterns during the dry and wet subperiods

To better understand the atmospheric and oceanic association with discharge anomalies in the Pantanal region, climatic behavior in specific subperiods was investigated. According to the general time evolution of discharge anomalies during the analyzed period, the whole period was divided in three subperiods following the mean signal anomaly of the Pantanal river discharge climatology (as indicated by the red vertical lines in Fig. 3): from 1970 to 1978, when negative anomalies are observed; from 1979 to 1995, period characterized by positive anomalies; and from 1996 to 2003, when river discharge anomalies became negative again. The maps to be presented forward represent the averaged atmospheric field over the characteristic rainy season (October to March) for the Pantanal region for each subperiod. In order to distinguish signals that contribute to define the climate of rainy season, this period was isolated.

Considering the interdecadal variability observed in the two first independent variables selected for simulation and prediction of the Pantanal discharge (mean SST at subtropical and tropical North Pacific), a possible PDO association with the SA precipitation was analyzed (Fig. 7). Although the mean SST at subtropical and tropical North Pacific areas do not exactly coincide with the PDO action centers (the one indicated by Latif and Barnett, 1994), the linear correlation spatial pattern between Pantanal discharge and SST over the Pacific basin, showing areas with negative and positive signs, is quite similar to PDO pattern. Minobe (1997),
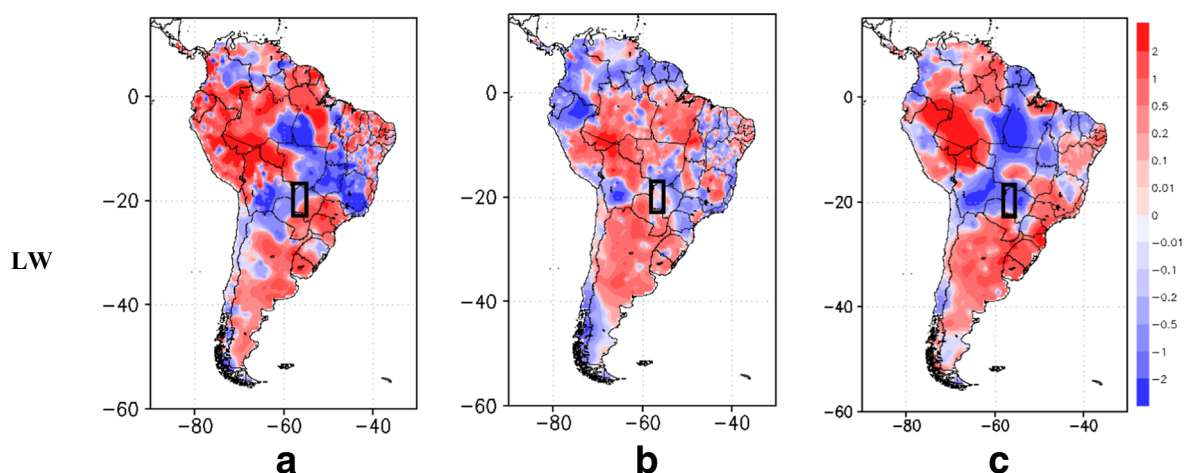

Fig. 6 South America precipitation anomaly (mm day^{-1}) from LW dataset for each subperiod **a** 1970–1977, **b** 1978–1996, and **c** 1997–2003. The Pantanal region is marked with a *black rectangle*
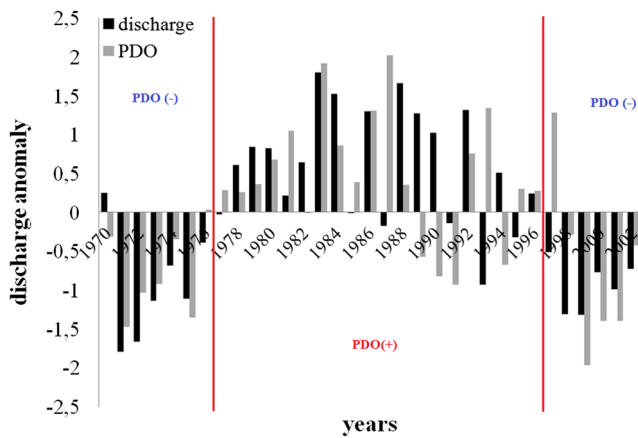
Fig. 7 Annual PDO index (Mantua et al. 1997) and Pantanal river discharge normalized anomalies from 1970 to 2003

Mantua (1999), and Mantua and Hare (2002) associated the 1970–1977 (1st subperiod in this study) and the 1997–2003 (3rd subperiod) periods with PDO negative phases and the 1978–1996 period (2nd subperiod in this study) to PDO positive phase. The statistical results found here, Fig. 7, suggest that positive (negative) PDO phases are associated with positive (negative) discharge and precipitation anomalies in the Pantanal region. While the association between river discharge and PDO seems to be quite significant ($r = 0.546$), as shown in Fig. 7, the association with precipitation (LW data) is less clear (Figs. 6 and 8). The monthly linear correlation map, Fig. 8, does not help to clearly identify positive correlation between precipitation in the Pantanal region and PDO index. Negative and positive correlation signs are observed over the studied area
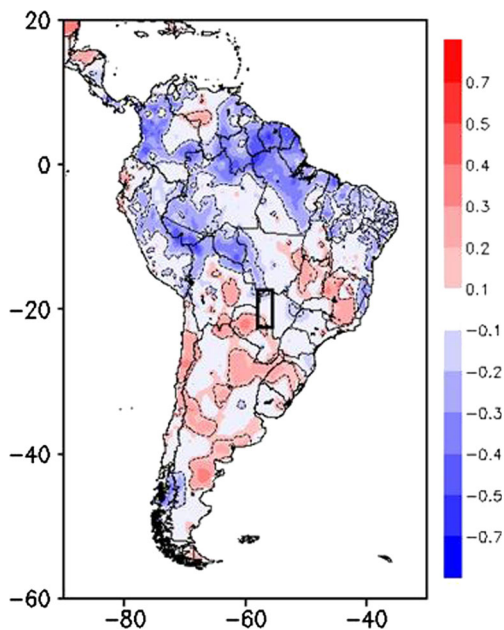

Fig. 8 Linear correlation between PDO index and South America LW precipitation, both in monthly resolution, from 1970 to 2003. Correlation with statistical significance of 99 % is shown inside *dashed lines*. Pantanal region is marked by the *black rectangle*

(Fig. 8), resulting in a negative mean correlation ($r = -0.3$). The linear correlation pattern, considering the PDO index, obtained for South America, is in agreement with Mantua and Hare (2002) results, who also used LW precipitation, but for the 1950–1996 period.

Divergence of humidity flux vertically integrated at low tropospheric levels (1000–700 hPa) (Fig. 9) was analyzed in each subperiod in order to understand the predominant atmospheric patterns established over SA, particularly over the Pantanal region. During the dry subperiods, 1st and 3rd, the mean anomaly divergence of humidity flux at low levels (1000–700 hPa) is positive (Fig. 9a, c) over the Pantanal region, with mean values equal to 0.5072×10^{-8} kg m^{-2} s^{-1} and 0.0491×10^{-8} kg m^{-2} s^{-1}, respectively, favoring drier conditions. During the wetter 2nd subperiod, the negative mean value (-0.2295×10^{-8} kg m^{-2} s^{-1}) indicates humidity convergence anomaly (Fig. 9b), favoring wetter climate conditions.

Distinct anomalous patterns at each subperiod defined by vector wind are observed at low levels (850 hPa) during rainy seasons, Fig. 10. Statistical significance at the level 90 % is observed in many areas when it is computed for zonal and meridional wind components anomalies (figures not shown). In the 1st and 3rd subperiods (drier conditions), anticyclonic anomalies centered at east central SA are observed, around 50º W, 18º S (marked with a yellow star in Fig. 10), embracing a large part of eastern Brazil. For the 3rd subperiod, a small cyclonic anomaly at the central part of this region is observed, but the anticyclonic anomalies are dominant. The anticyclonic anomaly observed for the 3st subperiod is less evident than for the 1st subperiod. The 2nd subperiod, else, presents a distinct anomalous circulation pattern in relation to the 1st and 3rd subperiods. It shows the climatological northerly circulation weakening over the central of SA, covering Mato Grosso do Sul, Mato Grosso, Pará and eastern Amazonas State. Besides that, the 2nd subperiod shows a cyclonic anomaly over the northeast portion of SA (marked by a red star in Fig. 10b), to the north of the circulation anomalous center displayed in the 1st and 3rd subperiods. The anomalous circulation observed in the 2nd subperiod contributes to the northerly circulation weakening. Thus, while the 1st and 3rd subperiods, characterized by drier climates for the Pantanal region, show the northerly low level circulation strengthening in the central SA region, the 2nd subperiod shows a weakened low level circulation. This result suggests a relationship between the moisture availability in the Pantanal region and the northerly low level circulation intensity in climatic scales.

In order to better understand the predominant circulation over South America and the possible influence from any Pacific forcing, mean fields for filtered geopotential height and stream function anomalies at high levels were analyzed. For the 1st and 3rd subperiods (drier conditions), positive geopotential height and anticyclonic anomalies over the Brazilian southeast region and adjacent South Atlantic
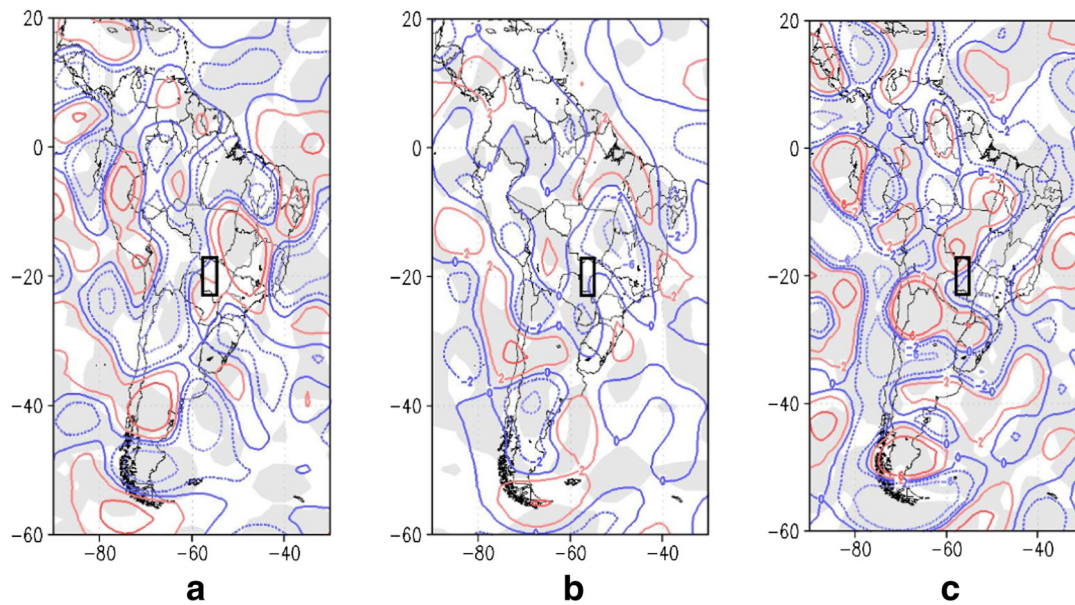
Fig. 9 Divergence of humidity flux vertically integrated (10^{-8} kg m^{-2} s^{-1}) at 1000–700 hPa for the **a** 1st, **b** 2nd, and **c** 3rd subperiods. Significant areas, at the 90 % level, are *shaded in gray*. The Pantanal region is marked with a *black rectangle*

Ocean were observed (Figs. 11a, c), while for the 2nd subperiod (wetter condition), the opposite sign was observed: negative geopotential height and cyclonic anomalies over the same region (Fig. 11b). Positive (negative) geopotential anomalies are commonly related to ridge amplification leading to drier (wetter) conditions under a barotropic atmosphere. In the three subperiods, atmospheric patterns associated with Rossby wave propagation can be seen coming from the South

Pacific basin similarly to the Pacific South America (PSA) pattern, as shown by Mo and Ghil (1987) and Szeredi and Karoly (1987a, 1987b). This result could suggest the relationship between climatic patterns over southeastern South America regions and Pacific Equatorial conditions in decadal scale, due to large periods characterized by distinct PDO anomalies as considered in this study (1970–1976, 1977–1996 and 1997–2003).
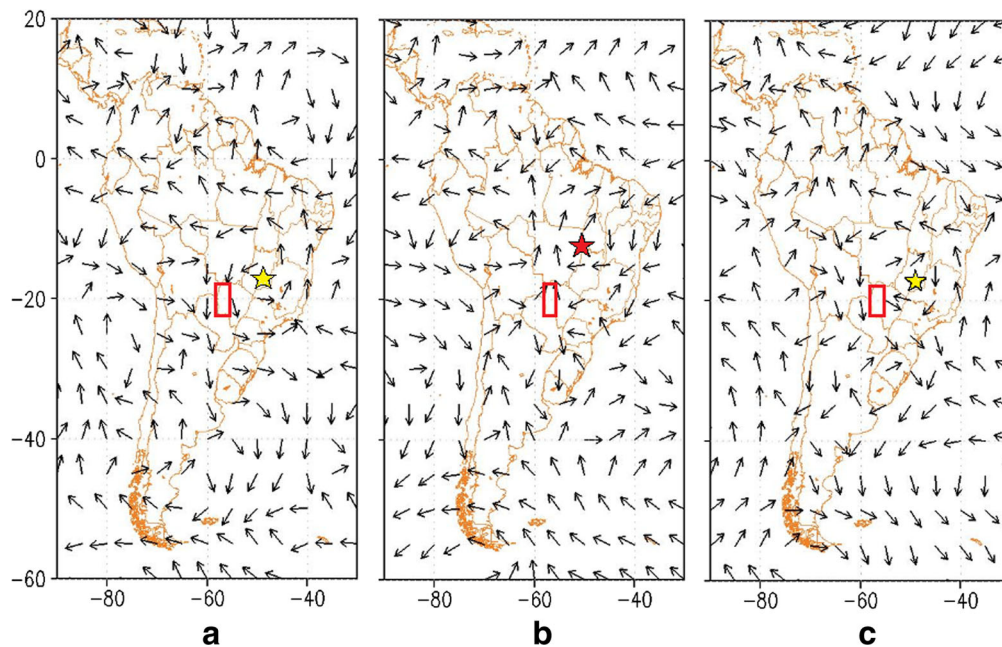

Fig. 10 Vector wind anomaly at 850 hPa for the **a** 1st, **b** 2nd, and **c** 3rd subperiods. The *yellow star* marks the center of the anomalous anticyclonic region over the eastern SA for the 1st and 3rd subperiods.

The *red star* marks the center of the anomalous cyclonic region for the 2nd subperiod. The Pantanal region is marked with a *red rectangle*
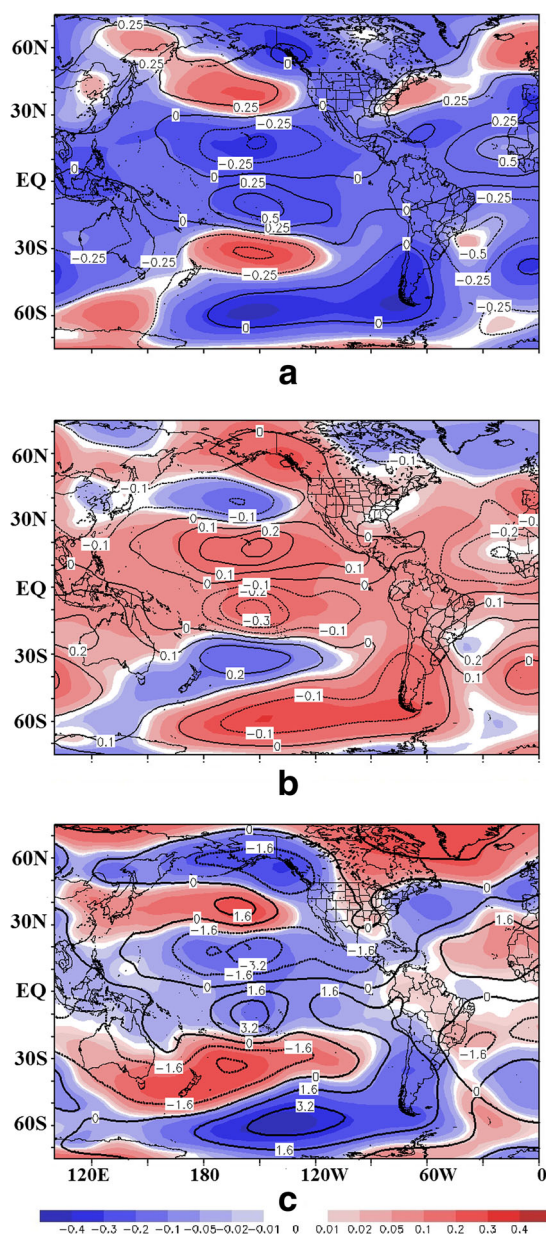
Fig. 11 Geopotential height (10^2 mgp) (*shaded*) and stream function filtered (10^7 m^2 s^{-1}) (*contour lines*) (low frequency) anomalies at 250 hPa and 0.21 sigma level, respectively, for **a** 1st, **b** 2nd, and **c** 3rd subperiods. The 1st and 2nd subperiods (3rd subperiod) present statistical significance, at the 90 % (75 %) level, for areas with absolute values of geopotential height and stream function anomalies above 0.1×10^2 mgp and 0.2×10^7 m^2 s^{-1}, respectively

4 Discussion and Conclusion

In this study, the linear relationship between sea surface temperature over oceans worldwide and river discharge in the center of South America, particularly in the Pantanal region, was analyzed. In addition, the climatic patterns associated with negative and positive anomalies of river discharge at the selected region were also investigated. The results indicate relevant linear correlations between Pantanal and a large part of the Pacific basin. Over the Atlantic Ocean, significant correlation was observed in the southeast portion of the South Atlantic and over the north of the North Atlantic, in high latitudes. The Pacific areas with high correlation with discharge in the Pantanal region are those away from the classic ENSO regions. In the "horseshoe" patterns over the Pacific, the inner (eastern) correlation sign is positive while the outside sign (western) is negative. The linear sign reaches relatively high values in many areas, ranging from 0.4 to 0.6, which is persistent in space and time, when lagged correlations are considered. The correlation patterns obtained by original data (without smoothing) are similar to those obtained by smoothened data, but with smaller absolute values.

Although the north and the south Pacific present almost the same spatial pattern for correlation values, the strongest values (both negative and positive) are found over the North Pacific, at subtropical and tropical areas. Even in the southeast of the South Pacific, the adjacent area to the west coast of SA, a persistent positive correlation signal is observed, which is similar to the first EOF mode obtained by many authors (e.g., Deser et al. 2010; Kawamura 1994; Smith et al. 1996). The southeast sector of the South Atlantic also presents important linear positive signal in relation to the river discharge in Pantanal. In fact, the South Atlantic area is sometimes related to the climatic variability over South America central areas through the South Atlantic Convergence Zone (SACZ) north/south displacement during rainy seasons (e.g., Robertson and Mechoso 2000). The north of the North Atlantic also presents significant negative linear correlation to Pantanal discharge, corroborated by EOF patterns applied on Atlantic SST (Weare and Newell 1977). Since cold (warm) anomalies in the tropical North Atlantic are related to the strengthening (weakening) of northeast trade winds, the variability of trade winds from northeast can be, in its turn, associated with SST climatic anomalies over the north of the North Atlantic, what must be verified in future studies.

The strengthening/weakening of the northeast trade winds over tropical North Atlantic (TNA) can intensify/weaken the moisture advection from tropical Atlantic into SA (Hastenrath 1978; Hastenrath and Heller 1977; Moura and Shukla 1981), which can also be associated with the meridional SST gradient over the tropical Atlantic. Even considering these statements, atmospheric circulation in the center of SA does not seem directly related to TNA SST. In general, no significant values are found in the correlation maps for the tropical North Atlantic area.

Taking into account the oceanic areas which are well correlated to river discharge in the Pantanal hydrologic basin, a simulated discharge through linear adjustment, in annual and month scales, was calculated. The mean SST in the SNP, TNP, ESP, and ENA constituted the set of independent variables selected by the linear adjustment to simulate discharge in

annual scale. These variables explained, together, 51 % of the variance observed in annual Pantanal river discharge. In monthly scale, 66 % of the observed variance was explained by mean SST placed at the same areas mentioned above, but also considering the southeastern South Atlantic area. For a prediction approach of the Pantanal river discharge with 3 months ahead of SST values, the mean error provided by the developed model is equal to 35 % (accuracy equal to 65 %). Assuming a linear approach, the elaborated linear model presented a significant performance for seasonal discharge forecasts. This kind of results could be applied particularly to the management of hydropower generation in South America. The linear adjusts considering smoothed data are better than those with the original data, showing greater R^2. Even though, the 12-month running mean applied to the original data must remove part of the seasonal signal.

The analysis showing mean anomalies of humidity flux divergence (convergence) at low levels (1000 to 700 hPa) and circulation at 850 hPa during rainy seasons in the Pantanal region helped to explain the occurrence of drier (wetter) conditions, observed during the 1st (1970–1976) and 3rd (1996–2003) subperiods (2nd subperiod, 1977–1995). The drier and wetter subperiods were respectively characterized by intensification and weakening of northerly flow at 850 hPa over the center of SA. Drier periods (1st and 3rd), which concomitantly occurred with PDO negative phases, are characterized by anticyclonic anomalies at 850 hPa over east central South America.

Geopotential high and stream function filtered data (low pass) indicated interesting features. Southeastern South America and the adjacent South Atlantic Ocean show geopotential high and stream function with positive and negative values for the drier subperiods (1st and 3rd). During the wetter subperiod (2nd), the signs over the same region are the opposite, but with a similar wave pattern. In fact, looking at the South Pacific circulation pattern, Rossby wave trains with opposite signs are visible during wetter and drier subperiods for the Brazilian Pantanal region. It is interesting to notice that the subperiods analyzed here coincide with different phases of PDO. Based on the results above, it would be conceivable to suggest that the PDO phases can be associated with distinct patterns of Rossby wave propagation throughout the South Pacific, therefore contributing to influence characteristic climatic patterns over the southeast region of South America. However, further analyses are still necessary in order to make this conclusion more robust.

References

Ab'Saber, AN (1939) O Pantanal Mato-grossense e a Teoria dos Refúgios. Revista Brasileira de Geografia. IBGE. Ano 1, N° 1 (Janeiro/março 1939). Rio de Janeiro, p. 9-57 (in portuguese)

Aceituno P (1988) On the functioning of the southern oscillation in the South American sector. Part I: surface climate. Mon Weather Rev 116:505–524

Bjerknes J (1969) Atmospheric teleconnections from the Equatorial Pacific. Mon Weather Rev 97:163–172

Camilloni I, Barros V (2000) The Paraná River Response to El Niño 1982–83 and 1997–98 Events. J Hydrometeorol 10:412–430

Cardoso AO, Silva Dias PL (2006) The relationship between ENSO and Paraná River flow. Adv Geosci 6:189–193

Cardoso AO, Silva Dias PL, Chamrro L (2004) O uso de TSM e vazão como preditores de vazão no Rio Paraná. CBMET – Anais do Congresso Brasileiro de Meteorologia, Fortaleza in portuguese

Castillo R, Nieto R, Drumond A, Gimeno L (2014) The role of the ENSO cycle in the modulation of moisture transport from major oceanic moisture sources. Water Resour Res 50(2):1046–1058

Coelho CAS, Uvo CB, Ambrizzi T (2002) Exploring the impacts of the Tropical Pacific SST on the precipitation patterns over South America during ENSO periods. Theory Appl Climatol Aust 71: 185–197

Deser C, Alexander MA, Xie SP, Phillips AS (2010) Sea surface temperature variability: patterns and mechanisms. Ann Rev Mar Sci 2:115–143

Drumond ARM, Ambrizzi T (2003) Estudo observacional e numérico da variação da circulação atmosférica nas Américas em episódios extremos da Oscilação Sul. Revista Brasileira de Meteorologia, São Paulo 18:1–12

Drumond ARM, Ambrizzi T (2008) The role of the South Indian and Pacific oceans in South American monsoon variability. Theor Appl Climatol 94:125–137

Drumond ARM, Amrbizzi T (2005) The role of SST on the South American atmospheric circulation during January, February and March 2001. Clim Dyn 781-791. doi:10.1007/s00382-004-0472-3

Duchon CE (1979) Lanczos filtering in one and two dimensions. J Appl Meteorol 18(8):1016–1022

Fernandez JPR, Franchito SH, Rao VB (2006) Simulation of the summer circulation over South America by two Regional Climate Models. Part I: Mean climatology. Theor Appl Climatol 86:247–260

Genta JL, Iribarren GP, Mechoso CR (1998) A recent increasing trend in the streamflow of rivers in southeastern South America. J Clim 11: 2858–2862

Gershunov A, Barnett TP (1998) Interdecadal modulation of ENSO teleconnections. Bull of the Am Meteorol Soc 79(12):2715–2725

Gillett NP, Kell TD, Jones PD (2006) Regional climate impacts of the Southern Annular Mode. Geophys Res Lett 33:L23704. doi:10.1029/2006GL02772

Gong D, Wang S (1999) Definition of Antarctic oscillation index. Geophys Res Lett 26(4):459–462

Hare SR, Francis RC (1995) Climate change and salmon production in the Northeast Pacific Ocean. Can Spec Publ of Fish and Aquat Sci 357–372

Hastenrath S (1978) On modes of tropical circulation climate anomalies. J Amos ScL 35:2222–2231

Hastenrath S, Heller L (1977) Dynamics of climatic hazards in northeast Brazil. Q J R Meteorol Soc 107:77–92

Hoskins BJ, Karoly DL (1981) The steady linear response of a spherical atmosphere to thermal and orographic forcing. J Atmos Sci 38: 1179–1196

Hurrell JW (1995) Decadal trends in the North Atlantic Oscillation: regional temperatures and precipitation. Science 269:676–679

Kalnay E, Kanamitsu M, Kistler R, Collins W, Deaven D, Gandin L, Zhu Y (1996) The NCEP/NCAR 40-year reanalysis project. Bull of the Am Meteorol Soc 77(3):437–471

Kao HY, Yu JY (2009) Contrasting eastern-pacific and central-Pacific types of ENSO. J Clim 22:615–632

Kaplan A, Cane MAY, Kushnir AC, Benno CM, Rajagoplan BB (1998) Analyses of global sea surface temperature 1856–1991. J Geophys Res 103:18567–18589. doi:10.1029/97JC1736

Kawamura R (1994) A rotated EOF analysis of global sea surface temperature variability with interannual and interdecadal scales. J Phys Oceanogr 24(3):707–715

Kiladis GN, van Loon H (1988) The southern oscillation. Part VII: Meteorological anomalies over the Indian and Pacific sectors associated with the extremes of the oscillation. Mon Weather Rev 116(1):120–136

Kousky VE, Kagano MT, Cavalcanti IFA (1984) A review of the southern oscillation: oceanic-atmospheric circulation changes and related rainfall anomalies. Tellus 36(A):490–504

Latif M, Barnett TP (1994) Causes of decadal climate variability over the North Pacific and North America. Science 266(5185):634–637

Latif M, Barnett TP (1996) Decadal climate variability over the North Pacific and North America: Dynamics and predictability. J of Clim 9(10):2407–2423

Legates DR, Willmott CJ (1990) Mean seasonal and spatial variability in gauge corrected, global precipitation. Int J Climatol 10:111–127

Magaña V, Ambrizzi T (2005) Climate variability in the tropical and subtropical Americas and El Niño/Southern Oscillation. Atmosfera 18:211–235

Mantua NJ (1999) The Pacific decadal oscillation and climate forecasting for North America. Climate Risk Solutions, 1(1):10–13.

Mantua NJ, Hare SR (2002) The Pacific Decadal Oscillation. J Oceanogr 58:35–44

Mantua NJ, Hare SR, Zhang Y, Wallace JM, Francis RC (1997) A Pacific interdecadal climate oscillation with impacts on salmon production. Bull Am Meteorol Soc 78:1069–1079. doi:10.1175/15200477

McPhaden MJ (2002) El Niño and La Niña: causes and global consequences. Encycl of Global Environ Chang, 1:353–370

Minobe S (1997) A 50-70 year climatic oscillation over the North Pacific and North America. Geophys Res Lett 24:683–686

Mo KC, Ghil M (1987) Statistics and dynamics of persistent anomalies. J Atmos Sci 144:808–823

Moura AD, Shukla J (1981) On the dynamics of droughts in northeast Brazil: observations, theory and numerical experiments with a GCM. J Atmos Sci 38:2653–2675

Müller GV, Ambrizzi T (2007) Teleconnection patterns and Rossby wave propagation associated to generalized frosts over southern South America. Clim Dyn 29:633–645

Nitta T, Yamada S (1989) Recent warming of tropical sea surface temperature and its relationship to the Northern Hemisphere circulation. J Meteor Soc Japan 67(3):375–383

Pinheiro F, Diniz IR, Coelho D, Bandeira MPS (2002) Seasonal pattern of insect abundance in the Brazilian Cerrado. Aust Ecol 27:132–136

Pinto MN (1988) Geomorfologia do Pantanal Matogrossense. Estudos e projetos de engenharia. Engevix S.A., p.78-85. Universidade de Brasília. Departamento de Geografia, Brasília

Quinn WH, Neal VT (1984) Recent climate change and the 1982–83 El Nino. In: Proc. eighth annual climate diagnostic workshop, Downsville, ON, Canada, NOAA, pp 148–154

Quinn WH, Neal VT (1985) Recent long-term climate change over the eastern tropical and subtropical Pacific and its ramifications. In: Proc. ninth annual climate diagnostic workshop, pp 101–109

Quinn WH, Zopf DO, Short KS, Kuo Yang RTW (1978) Historical trends and statistics of the Southern Oscillation, El Niño, and Indonesian drought. Fish Bull 76:663–678.

Rao VB, Hada K (1990) Characteristics of rainfall over Brazil: annual variations and connections with the Southern Oscillation. Theor Appl Climatol 42:81–91

Rao VB, Satyamurty P, Brito JIO (1986) On the 1983 drought in Northeast Brasil. J Climatol 6:43–51

Rayner NA, Parker DE, Horton EB, Folland CK, Alexander LV, Rowell D, Kaplan A (2003) Global analyses of sea surface temperature, sea ice, and night marine air temperature since the late nineteenth century. J of Geophys Res: Atmos, 108(D14)

Reboita MS, Ambrizzi T, Rocha RP (2009) Relationship between the Southern Annular Mode and Southern Hemisphere Atmospheric Systems. Revista Brasileira de Meteorologia 24(1):48–55

Robertson AW, Mechoso CR (1998) Interannual and decadal cycles in river flows oh southeastrn South America. J Clim 11:2570–2581

Robertson AW, Mechoso CR (2000) Interannual and interdecadal variability of the South Atlantic Convergence Zone. Mon Weather Rev 128:2947–2957

Ropelewski CF, Halpert MS (1989) Precipitation patterns associated with the high index phase of the Southern Oscillation. J Clim 2:268–284

Saji NH, Ambrizzi T, Ferraz ST (2005) Indian Ocean Dipole mode events and austral surface air temperature anomalies. Dyn Atmos Oceans 39:87–101

Smith TM, Reynolds RW, Livezey RE, Stokes DC (1996) Reconstruction of historical sea surface temperatures using empirical orthogonal functions. J Clim 9:1403–1420

Souza CA, Lani JL and Sousa JB (2006) Origem e evolução do Pantanal Mato-grossense. VI Simpósio Nacional de Geomorfologia-Reginal Conference on Geomorphology (1-11, 2006) (in portuguese)

Szeredi I, Karoly D (1987a) The vertical structure of monthly fluctuations of the Southern Hemisphere troposphere. Aust Meteorol Mag 35:19–30

Szeredi I, Karoly D (1987b) The horizontal structure of monthly fluctuations of the Southern Hemisphere troposphere from station data. Aust Meteorol Mag 35:119–129

Taschetto A, Ambrizzi T (2012) Can Indian Ocean SST anomalies influence South American rainfall? Clim Dyn 38:7–8

Trenberth KE (1984) Signal versus noise in the Southern Oscillation. Mon Weather Rev 112(2):326–332

Trenberth KE (1997) The definition of el nino. Bull of the Am Meteorol Soc 78(12):2771–2777

Trenberth KE, Hoar TJ (1996) The 1990–1995 El Niño-Southern Oscillation event: Longest on record. Geophys Res Lett 23(1):57–60

Trenberth KE, Hoar TJ (1997) El Niño and climate change. Geophys Res Lett 24(23):3057–3060

Trenberth KE, Stepaniak DP (2001) Indices of El Niño evolution. J Clim 14(8):1697–1701

Uvo CB, Repelli CA, Zebiak SE, Kushnir Y (1998) The relationships between tropical Pacific and Atlantic SST and northeast Brazil monthly precipitation. J Clim 11(4):551–562

van Loon H, Roger JC (1978) The seesaw in winter temperatures between Greenland and northern Europe. Part I: General description. Mon Wea Rev 106:296–310

Vera C, Higgins W, Amador J, Ambrizzi T, Garreaud R, Gochis D, Zhang C (2006) Toward a unified view of the American monsoon systems. J Clim 19(20):4977–5000

Walker GT (1924) Correlation in seasonal of weather. Memoirs of the India Meteorological Department. V. XXIX

Walker GT, Bliss EM (1932) World Weather. V Mem Roy Meteor Soc 4: 53–84

Weare BC, Newell RE (1977) Empirical orthogonal analysis of Atlantic Ocean surface temperatures. Q J R Meteorol Soc 103(437):467–478

Weare BC, Navato AR, Newell RE (1976) Empirical orthogonal analysis of Pacific sea surface temperatures. J Phys Oceanogr 6(5):671–678

Wilks DS (1995) Statistical Methods in the Atmospheric Sciences: an introduction. Academic Press, San Diego, 467 p

Willmott CJ, Matsuura K (2005) Advantages of the mean absolute error (MAE) over the root mean square error (RMSE) in assessing average model performance. Clim Res 30:79–82

Zhang Y, Wallace JM, Battisti DS (1997) ENSO-like interdecadal variability: 1900-93. J Clim 10(5), 1004–1020

Zhou J, Lau KM (1998) Does a Monsoon climate exist over South America? J Clim 11(5):1020–1040